



Disposable Sleeping Mat

Design focused to provide a sleeping solution to the homeless community



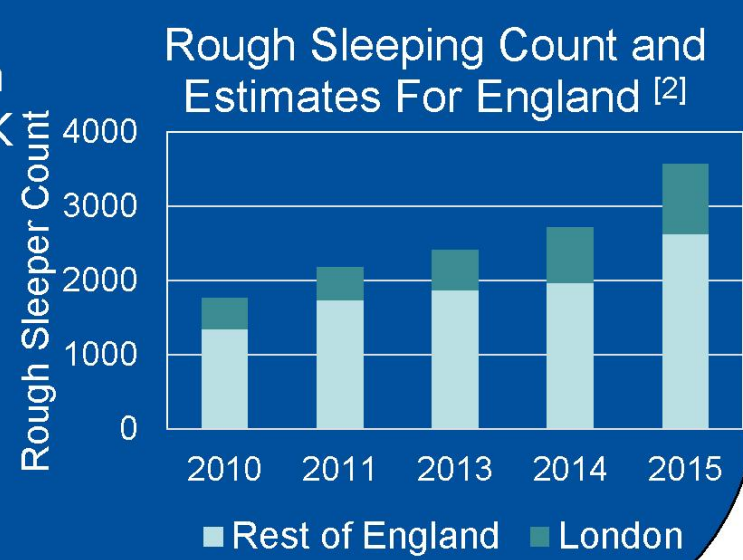
Project Background

Sleep is an essential biological need to sustain life. In disaster relief sleeping products are highly requested, but not always received.

The current housing crisis in the UK has led to a growing estimated rough sleeper population of 3,569 in England.

The average **age of death** of rough sleepers in the UK is just **47 years** for men and **43 years** for women.^[1]

A large factor to the low life expectancy are health issues attributed to street sleeping conditions.



Design Requirements Provided Free

There must be no material or manufacturing cost. Members of the homeless community have very little disposable income.

Strong, Comfortable and Warm

Rough sleepers encounter many health issues due to their sleeping conditions. The user needs to be supported above the unforgiving cold ground.

Compact and Portable

With nowhere to store possessions all sleeping apparatus have to be constantly carried or insecurely stashed away.

Quick Assembly

Imagine how frustrating it must be to have to build your bed every time you wanted to sleep.

Recyclable and Replaceable

The possessions of the homeless community often get lost, stolen or damaged. Councils would only allow mats to be provided if they will not pollute the local environment.

Survive outdoor conditions

The mat has to withstand the environment it is used in.

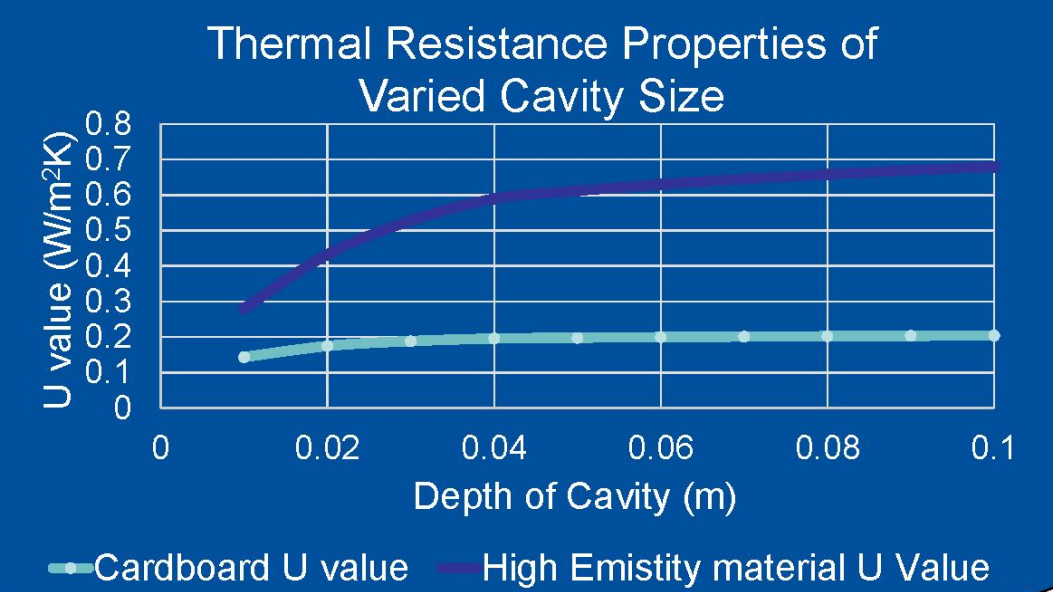
Thermal Properties

The sleeping mat needs the highest thermal resistance possible in order to protect users from varying ground temperatures.

Parameters that greatly effect thermal properties are the distance between objects of differing energy and the material that divided them.

Need to find the optimal trade off between pack size and thermal resistance.

The graph below used the calculation method for thermal resistance of building elements set out by the British standard institute^[4].



Final Design Solution

The mat will be free to anyone who needs it:

- The sleeping mat reuses cardboard from supermarkets and bike shops. It only requires four hot glue gun sticks.
- The manufacturing process only needs a Stanley Knife and a glue gun and can be done almost anywhere.
- The only manufacturing cost are for the hot glue gun sticks, which amounts to under 30p. This very low cost can be covered by volunteers.

Aesthetically the mat blends in to its environment:

- A big part of the feedback was that the design should not cause someone sleeping rough to stand out.
- Also if the design was too substantial there could be issues with local authorities.

The mat provides a 50mm clearance from the ground:

- This proved to be the optimal trade-off clearance between thermal properties and pack size.
- The lower lattice divides the cavity between the user and the ground into smaller sub sections. This restricts the circulation of air deterring convective heat loss.
- Provides a more forgiving sleeping surface for the user.



The mat is a short term solution and fully recyclable after use:

- The mat contains less than 1.5% contaminate materials and can therefore be fully recycled.
- The mat is aimed to be disposable and replaceable.

The mat spans a sleeping area of 200cm x 55cm and comfortably supports a person's weight:

- The mat has an adjustable length of up to 2 meters.
- The lower layer *kagome lattice* support structure distributes interconnecting supports evenly across the mats surface meaning it can easily support someone standing on the mat.
- There is an inclined head rest at the end.

The assembly and disassembly takes less the 30 seconds and requires no physical force:

- You simply pull out the lower lattice support and unfold the top layer slotting the legs into the sockets.
- The assembly is very intuitive and does not require instructions.

The mat compacts down into a lightweight and secure unit:

- When not in use the mat can be compacted down into a secure unit 630mm x 360mm x 110mm (Size of a bed pillow).
- There is a handle that can be used when the mat is in its compact state to make it more portable.
- The mat weighs less than 2kg.

Design Implementation

Manufacturing Process

- The cardboard sleeping mat consists of 42 parts, of which there are nine different independent parts.
- The manufacturing process is simple and repetitive.
- But it is also time consuming as one mat take 4 hours to construct.

Student Workshop

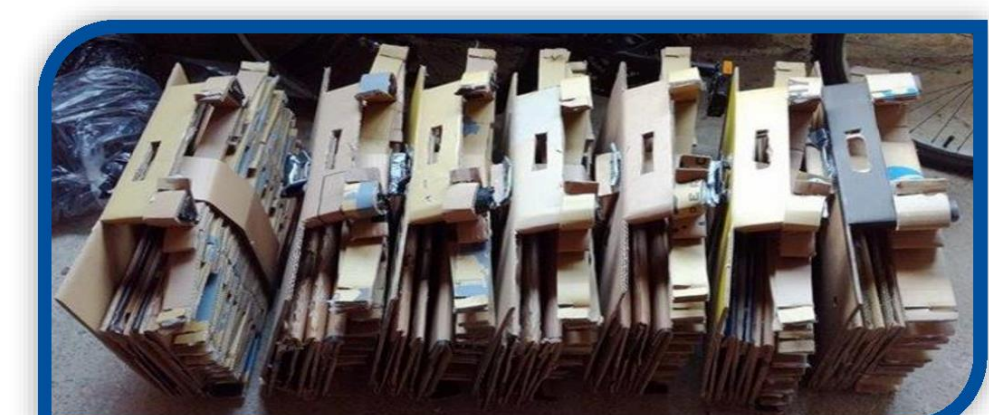
- A workshop was put on within the University of Exeter's engineering department.
- A group of student volunteers produced seven mats during the morning workshop.
- The mats are currently on trial at an Exeter based homeless charity, St Petrock's



Future Development Water Proofing

The mat is not waterproof, but neither is a sleeping bag. The packed down unit comfortably fits into a plastic bin bag meaning it can be stored without getting wet. Alternative materials are being investigated to achieve water proofing.

Other Areas For Development: Reduce Manufacturing Time Reduce Pack Size



Acknowledgement

- Antifreeze, Brighton
- St Petrock's, Exeter
- Dr Matthew Eames
- Exeter University Student workshop team
- Dr Philippe Young
- Dr Arnaud Marmier

Introduction

- The **aorta** is a large elastic artery which is a reservoir for blood ejected from the heart.¹
- With age, the aorta becomes **stiffer** and less **compliant**,¹ negatively affecting the heart and other downstream areas.^{2,3,4,5,6}
- The cerebral circulation usually attenuates the arterial waveform to prevent damage.⁸
- **Aortic stiffening** could amplify the pressure wave in the cerebral arteries^{9,10,11}
- High pressure fluctuations can cause harm, leading to **microhaemorrhages** and other damage.^{3,9,12,13}
- Carotid-femoral pulse wave velocity (**cf-PWV**) is the gold-standard to measure aortic stiffness,⁷ measuring the speed that the pulse wave travels from the heart to the femoral artery in the leg.
- Cf-PWV is calculated using the **SphygmoCor** (Fig. 1), which uses a pressure probe, or the **Vicorder** (Fig. 2), which uses inflatable cuffs, which record at carotid and femoral pulses.
- Transcranial Doppler ultrasound (**TCD**) is used to non-invasively examine **cerebral blood flow pulsatility**¹⁴ (Fig. 3).
- We examined the relationship between **aortic stiffness** and **cerebral artery pulsatility** in TIA/minor stroke patients, for whom downstream effects could be devastating.

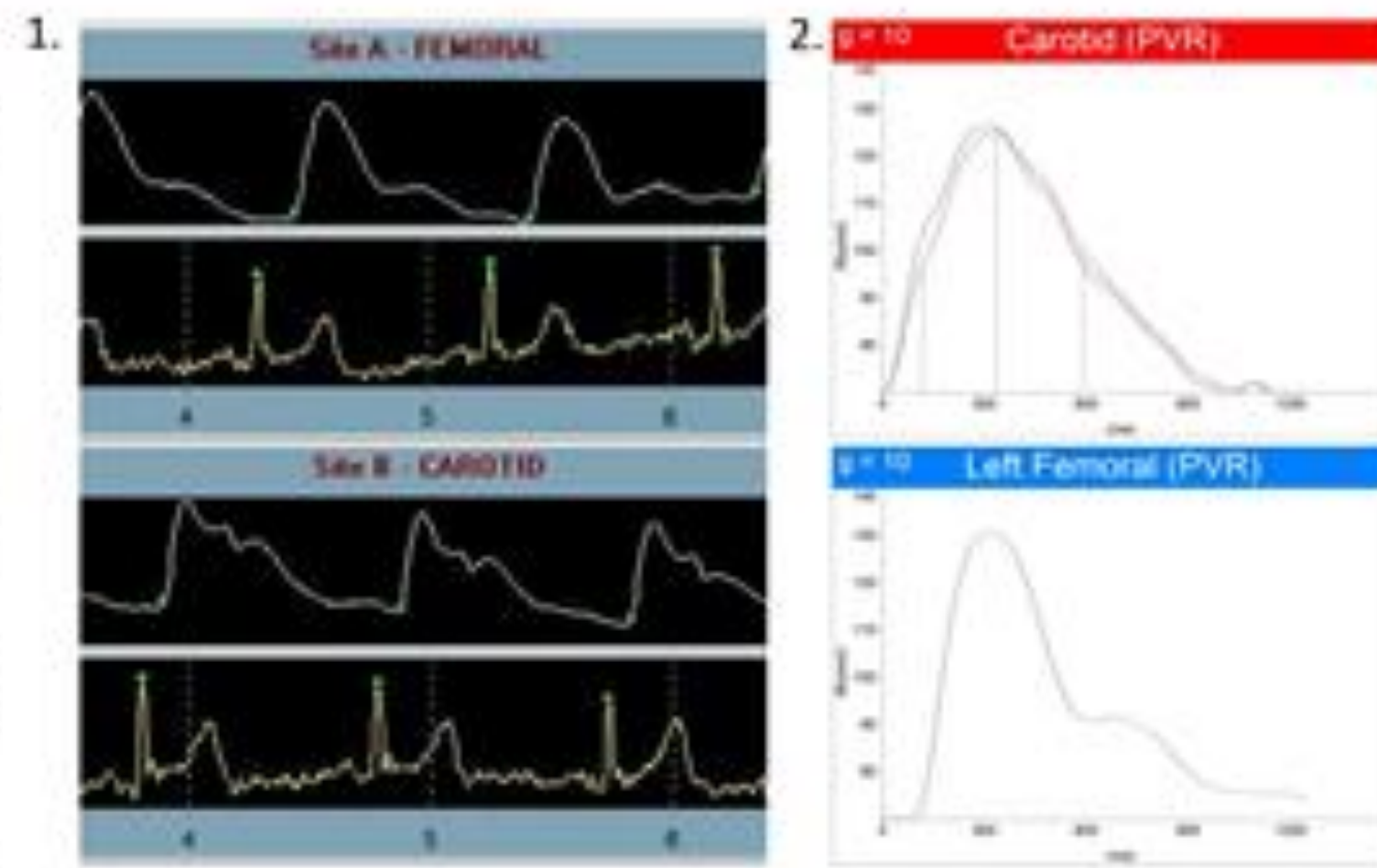


Figure 1: SphygmoCor cf-PWV graphs. x-axis: time (s), y-axis: arterial pressure fluctuations (mmHg). Upper graph shows femoral waveform, lower graph shows carotid waveform. Figures 1, 2 and 3 are from a single patient.

Figure 2: Vicorder cf-PWV graphs. x-axis: time (ms), y-axis: arterial pressure fluctuations (mmHg). Upper graph shows carotid waveform, lower graph shows femoral waveform.

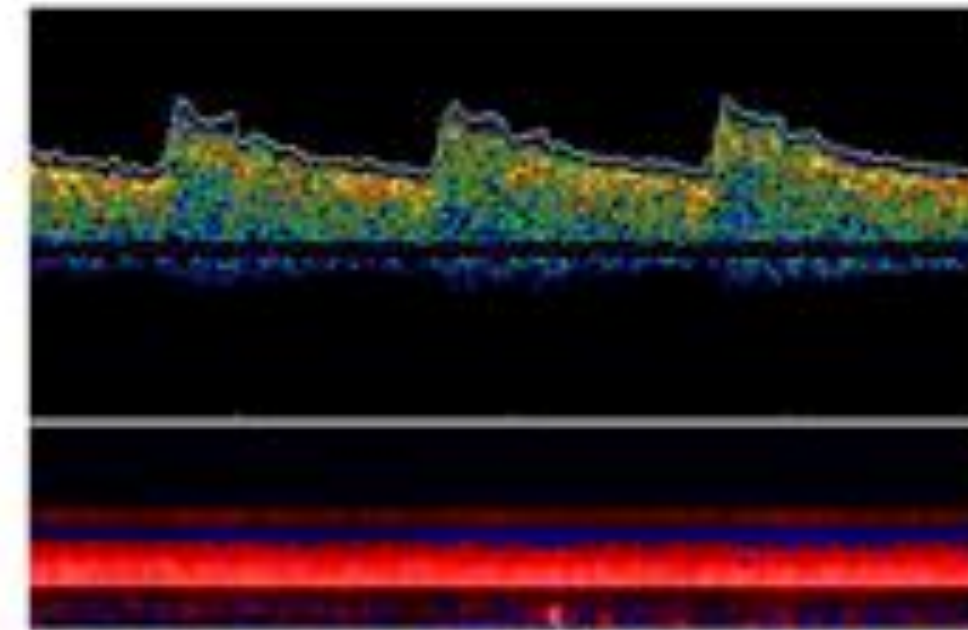


Figure 3: TCD waveform taken from the left middle cerebral artery. x-axis: time, y-axis: velocity. Below the graph is the M-mode, which shows the direction of blood flow in relation to the probe at different depths.

Aims & Hypothesis

Aim: to examine the relationship between **cerebral artery pulsatility** and **aortic stiffness** in **transient ischaemic attack (TIA)** and **minor stroke** patients.

Hypothesis: the pathophysiology of aortic stiffness is linked to increased cerebral artery pulsatility, so there will be a **strong positive correlation** between these two factors.

Methods

Participants were consenting **TIA** or **minor stroke** patients from the **Oxford Vascular Study**,¹⁵ seen at a clinic one month after their acute event. During recordings, patients lay supine without moving or speaking.¹³

The **SphygmoCor** uses the distances between the carotid and femoral arteries and the sternal notch, plus ECG-gated tonometry of the carotid and femoral artery waveforms to calculate cf-PWV.

The **Vicorder** uses inflatable cuffs attached to the neck and thigh, which were inflated to detect the pulse wave, as well as the distance between the thigh cuff and the sternal notch, to calculate cf-PWV.

TCD: Using a Doppler Box (Compumedics DWL, Singen, Germany), a 2MHz probe was held at 'acoustic windows' on the skull,¹⁴ and blood flow characteristics, such as the pulsatility index (PI), measured in the middle cerebral arteries (MCAs).

Statistical analysis: Using IBM SPSS Statistics 22, correlations were calculated between cf-PWV and MCA PI, and **adjusted for age**, a major confounding factor. Student's t-test was used to calculate significance of results. Significance level set at **p < 0.05**.

Results SphygmoCor cf-PWV

The age-adjusted correlation between mean MCA PI and mean SphygmoCor cf-PWV is **r = 0.647, p < 0.0005, N = 74**.

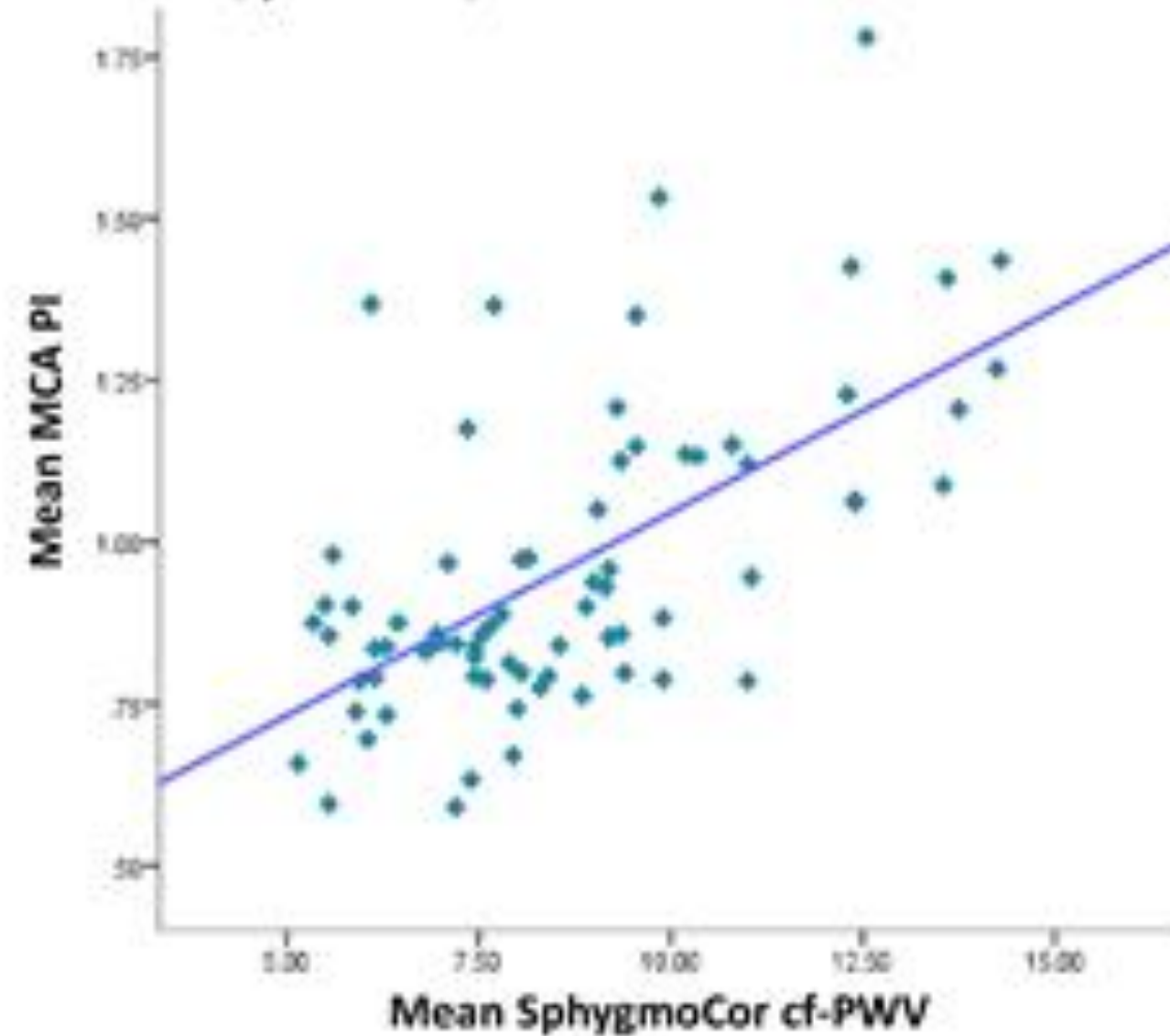


Fig. 4 shows the correlation between mean SphygmoCor cf-PWV and mean MCA PI. Using a linear best fit line, **R² = 0.393**.

Figure 4: A graph of the correlation between mean MCA PI and mean cf-PWV (as measured by the SphygmoCor). **R² linear = 0.393**. The linear best fit line is plotted.

Vicorder cf-PWV

The age-adjusted correlation between mean MCA PI and mean Vicorder cf-PWV is **r = 0.614, p = 0.036, N = 32**.

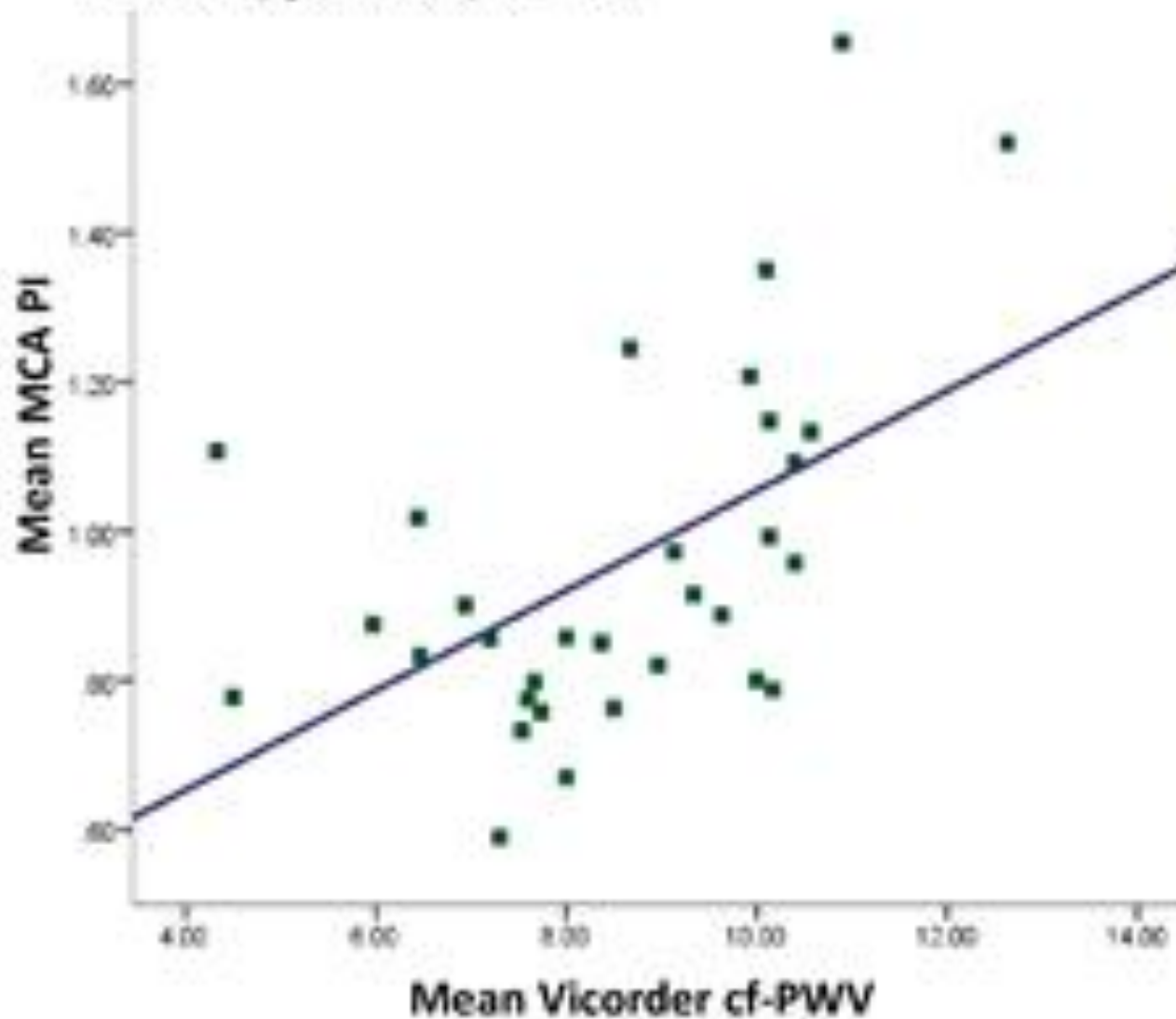


Fig. 5 shows the correlation between mean Vicorder cf-PWV and mean MCA PI. Using a linear best fit line, **R² = 0.273**.

Figure 5: A graph of the correlation between mean MCA PI and mean cf-PWV (as measured by the Vicorder). **R² linear = 0.273**. The linear best fit line is plotted.

These data show:

- **Strong, positive, linear correlation** between cf-PWV and MCA PI.
- Correlation is consistent for **both devices**, and when **adjusted for age**.
- **Significant relationship** between **aortic stiffness** and **cerebral artery pulsatility**.

Discussion

- The results of this study are in agreement with the results of prior studies.^{9,10,11,12}
- Despite the lower p and r values of the **Vicorder**, the relationship between these factors can be confidently accepted, as the **SphygmoCor** is more **well-validated** and measurements were carried out on more patients.
- A comparison of the **Vicorder** and **SphygmoCor** devices (author's own work, unpublished) showed that the two cf-PWV measures gave within-patient values that were not significantly different.

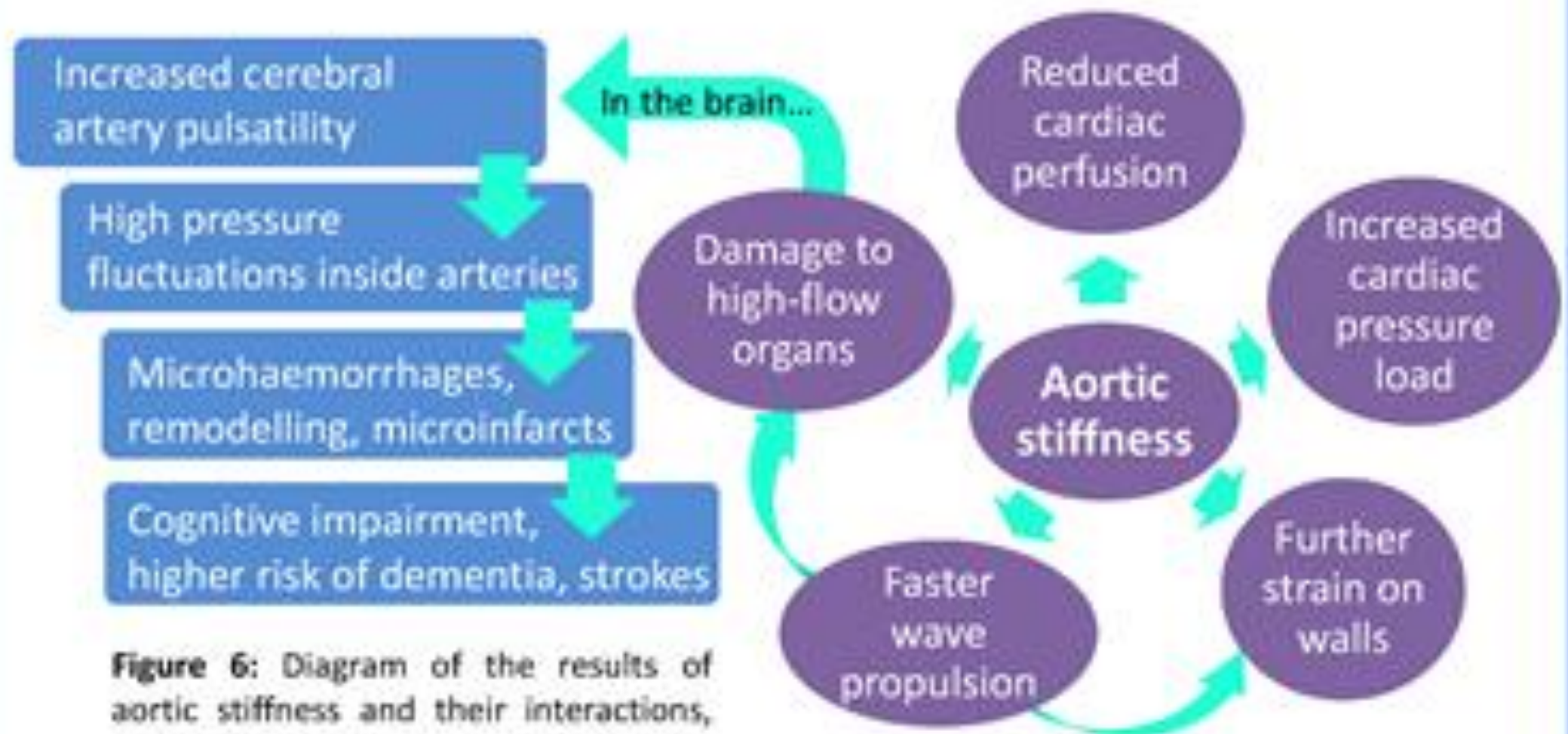


Figure 6: Diagram of the results of aortic stiffness and their interactions, and its effect on the cerebral circulation

- The downstream effects of **aortic stiffening** (Fig. 6) happen because the aorta cannot **absorb** and **reduce** the impact of blood pressure pulsations effectively.³
- The **turbulent pulse wave** moves more quickly into the **high-flow, low-resistance cerebral circulation**,¹² creating increased pulsatility in the cerebral arteries.
- Pulsatility increase leads to: cerebral artery rupture causing **microhaemorrhages**³ (small bleeds in the brain) and artery wall **remodelling**,¹² leading to **reduced arterial reactivity**.
- Reduced reactivity leads to **microinfarcts**¹² (small areas of cerebral ischaemia), which appear clinically as **cognitive impairment**, and an increased risk of **ischaemic stroke, haemorrhagic stroke and dementia**.^{3,11,12}
- **Stroke** and **TIA** patients have already experienced a **vascular event**, and may have significant cardiovascular pathology, so this relationship and its effects are troubling.²⁰
- It is important to be able to **predict future risk** of complications due to arterial stiffness and cerebral artery pulsatility.
- Monitoring changes in cf-PWV and concurrent changes in cerebral artery pulsatility, especially in TIA/stroke patients, could allow **early management** of changes, **maintain** patient health, and **prevent** further damage and disease.

References

1. Shirwany & Zou. *Acta Pharmacol Sin.* 2010;31(10):1267-1276
2. Tuttolomondo et al. *Atherosclerosis.* 2010;211(1):187-194
3. Adji et al. *Am J Hypertens.* 2011;24(1):5-17
4. Hamilton et al. *Clin Sci.* 2007; 113(4):157-170
5. Kaess et al. *JAMA - J Am Med Assoc.* 2012;308(9):875-881
6. Calvacante et al. *J Am Coll Cardiol.* 2011;57(14):1511-1522
7. Schubert T, et al. *Am J Neuroradiol.* 2011;32(6):1107-1112
8. Van Bortel et al. *J Hypertens.* 2012;30(3):445-448
9. Xu TY, et al. *Am J Hypertens.* 2012;25(3):319-324
10. Webb et al. *Stroke.* 2012;43:2631-2636
11. Kwate, et al. *Blood Pressure.* 2009;18(3):130-134
12. Mitchell GF, et al. *Brain.* 2011;134(11):3398-3407
13. Laurent et al. *Eur Heart J.* 2006;27(21):2588-2605
14. Alexandrov et al. *J Neuroimaging.* 2007;17(1):11-18
15. Li et al. *Lancet Neurol.* 2015;14: 903-913

Acknowledgements

With thanks to Dr. Louise Silver and Dr. Sara Mazzucco, Dr. Adam Lewandowski, Dr. Alastair Webb, Dr. Giulia Turri, Jonathan Diesch, and the rest of the OXVASC team.

THORIUM: A PATHWAY TO CLEAN NUCLEAR ENERGY

Researching the potential of Thorium as nuclear fuel in Liquid Fluoride Thorium Reactors and raising awareness for a safer and more advantageous alternative fuel to current nuclear power plants.

INTRODUCTION

Uranium is not the only radioactive element that can be used to create nuclear power. The alternative to it is a naturally occurring and slightly radioactive element named **Thorium (Th)**. By utilizing this element in a special **thorium-uranium cycle (Th-U)**, which works best in conjunction with a certain type of reactor called the **Liquid Fluoride Thorium Reactor (LFTR)**, many advantages over conventional nuclear power plants can be achieved.

The Generation IV International Forum has evaluated 130 reactor concepts and has selected six reactors for deployment between 2020 and 2030, of which one is the Molten Salt Reactor (also known as the LFTR, when used with thorium as the fuel) [1].

HOW LFTRS WORK

Uranium and thorium are dissolved in molten fluoride salts (e.g. beryllium and lithium), hence providing a **liquid fuel** that can operate at **low pressure** (no risk of explosion), as opposed to the conventional reactors that use water as the coolant. The liquid fuel produces nuclear reactions in the core and a blanket of thorium surrounding it, breeds more thorium into a fissile fuel.

ADVANTAGES OF THORIUM



REDUCES RADIOACTIVE WASTE BY A FACTOR OF 5000

Thorium produces less waste than traditional power plants. After 10 years 83% of the Th waste becomes safe and can be reprocessed, the rest 17% would become safe in the next 300 years, as opposed to 10,000+ years for uranium waste. It also produces zero CO₂ emissions [3].



LFTR SAFETY DESIGN

A meltdown is impossible in a LFTR. If there is a power outage, the frozen salt in the freeze plug would melt, giving way for the fuel to drain into a safety container.



CHEAPER THAN COAL

LFTR might be cheaper than traditional nuclear energy, and even coal. Since the LFTR operates at atmospheric pressure, the size of the power plant would be more compact, meaning that they could potentially be mass produced as small modular reactors [4].



1 TON OF THORIUM IS EQUIVALENT TO 200 TONS OF URANIUM

Thorium has a high energy yield. 1 ton of thorium produces an equivalent amount of energy to 200 tons of uranium or 3,500,000 tons of coal. This means 1 ton of thorium could provide power to 700,000 houses for a whole year [5].



3-4 TIMES MORE ABUNDANT THAN URANIUM

Thorium is found in most rocks and soils, and is a by-product of rare earth mining. It is plentiful even in the UK. There is enough to power the world for the next 10,000 + years. This in turn increases energy security [6].

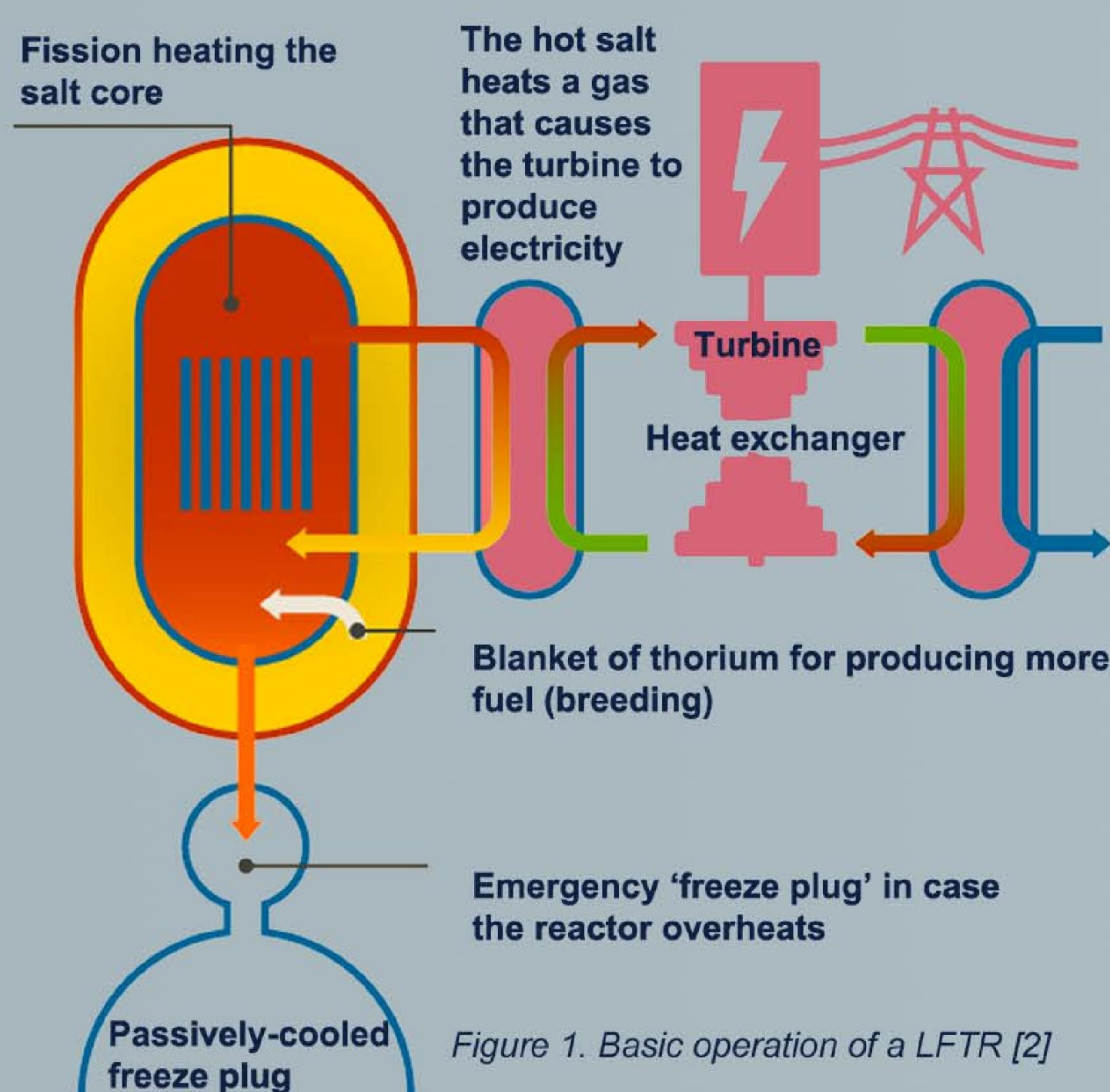


Figure 1. Basic operation of a LFTR [2]

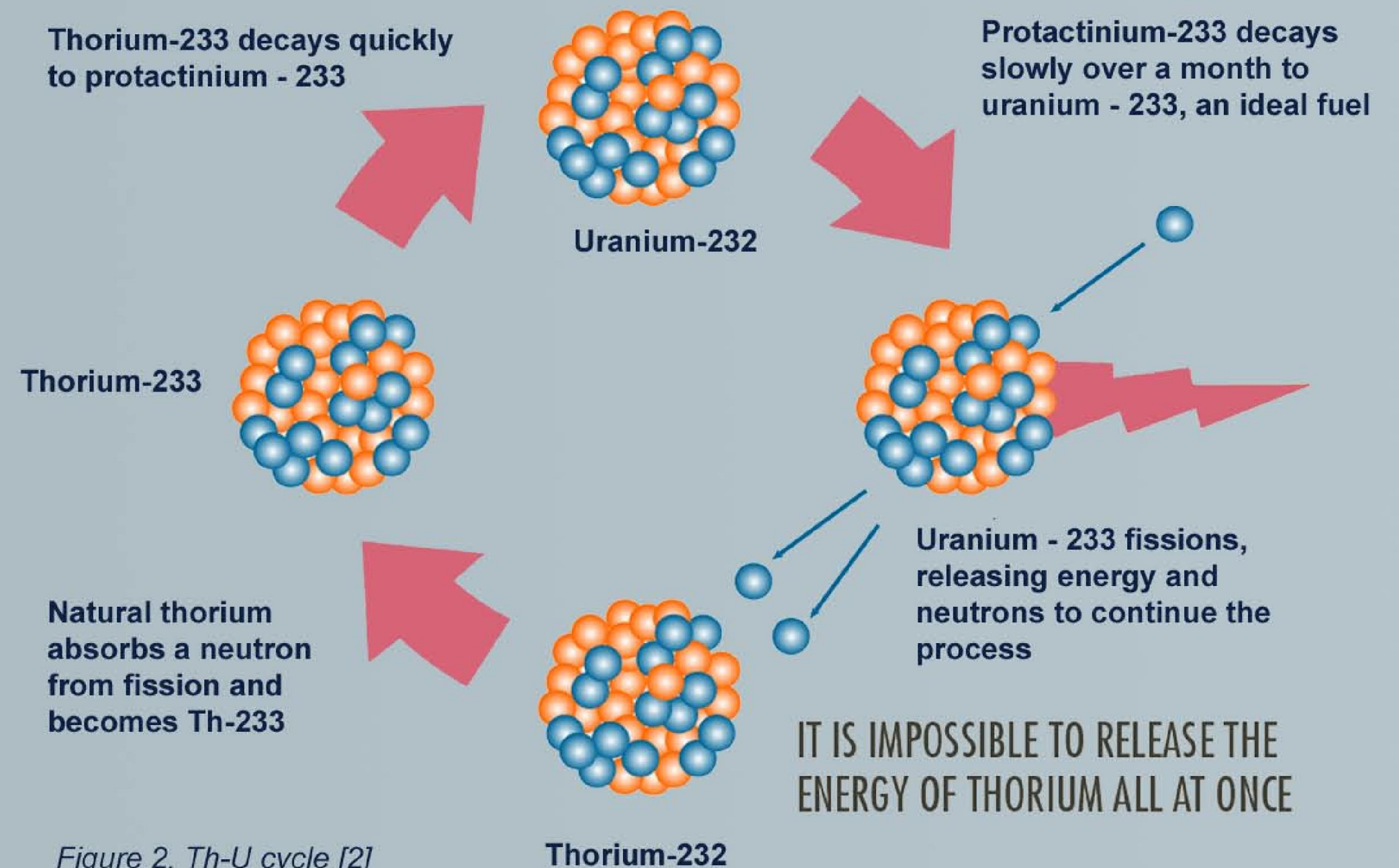


Figure 2. Th-U cycle [2]

THORIUM FUEL CYCLE

A (Th-U) fuel cycle needs Uranium or Plutonium to initiate a chain reaction since thorium is not a fissile material but fertile and generates fissile U-233 when absorbing a neutron. The fission of uranium produces 2 neutrons, one continues the chain reactions and the other goes on to transform more thorium atoms into uranium. Figure 2 demonstrates the cycle. The fission reaction takes place in the molten salt solution (instead of water), hence the reaction is more efficient avoiding a meltdown [2].

CONCLUSION

The research conducted suggests that thorium has the potential to address the energy trilemma. Energy security is not a problem as Thorium is just too common, even in the next thousands of years (as well as beyond then if sourced from other planets) there will be plenty of it. Energy equity can also be achieved as Thorium has a high energy density and can be sourced through mining dirt, which makes it economically practical. The environmental impact is significantly decreased, making it suitable for sustainable power production.

Sex Differences in Exercise Capacity in Children and Adolescents with Cystic Fibrosis

¹Children's Health & Exercise Research Centre, University of Exeter, UK; ²Royal Devon and Exeter NHS Foundation Trust Hospital, Exeter, UK; ³Faculty of Medicine, Dalhousie University, Halifax, Canada; ⁴Department of Sport & Exercise Science, University of Portsmouth, UK.

INTRODUCTION

- Females with cystic fibrosis (CF) have higher mortality rates than their male counterparts.⁽¹⁾
- Lung function (forced expiratory volume in 1 s - FEV₁) is a predictor of mortality.⁽²⁾
- Females still have a higher mortality rate when pulmonary function is removed as a factor.⁽³⁾
- Ventilatory efficiency at peak exercise (VE/VO₂ and VE/VCO₂) also shown to be predictive of mortality.⁽⁴⁾
- High exercise capacity (VO_{2max}) is a predictor of mortality independent of lung function, increases quality of life and reduces risk of hospitalisation for people with CF.⁽⁴⁾
- VO_{2max} is significantly different between sexes in healthy children.⁽⁵⁾
- However, it has yet to be determined whether a sex difference exists for VO_{2max} in CF populations.

AIM: To identify sex differences in exercise capacity in children and adolescents with CF after adjusting for body size, maturity and lung function

METHODS

- Cardiopulmonary exercise test (CPET) data collected from 24 participants with CF (14 males and 10 females) was retrospectively analysed.
- VO₂ data were scaled allometrically and by the ratio standard method for body surface area (m²), body mass (kg) and stature (cm).
- Mean, standard deviation and p values were calculated for lung function and exercise parameters using an independent samples T-test between males and females.
- Analysis of covariance (ANCOVA) were run independently for each scaled VO₂ to adjust for BMI (body mass index), FEV₁ and PHV (peak height velocity).



REFERENCES

- Corey et al. (1997) Longitudinal analysis of pulmonary function decline in patients with cystic fibrosis. *J Pediatr* 131:809-14.
- Kerem et al. (1992) Prediction of mortality in patients with CF. *N Engl J Med* 326:1187-91.
- Rosenfeld et al. (1997) Gender gap in CF mortality. *Am J Epidemiol* 145:794-803.
- Hulzebos et al. (2014) Prediction of mortality in adolescents with CF. *Med Sci Sports Exerc* 46:2047-52.
- McNarry et al. (2015) Aerobic function and muscle deoxygenation dynamics during ramp exercise in children. *Med Sci Sports Exerc* 47:1877-84.

RESULTS

Table 1. Descriptive Variables Including Lung Function Data

Variable	Male	Female	P value
Age (years)	13.7 ±3.0	12.6 ±3.0	0.41
BMI (kg/m ²)	21.7 ±3.9	18.9 ±2.6	0.06
Body mass (kg)	56.5 ±17.8	42.7 ±10.6	0.039*
BSA (m ²)	1.6 ±0.3	1.3 ±0.2	0.042*
Stature (cm)	159.5 ±14.3	149.1 ±12.1	0.08
PHV (years from)	-0.0 ±2.2	0.4 ±2.5	0.69
FVC (L)	3.6 ±1.3	2.6 ±0.5	0.044*
FVC (% predicted)	96.3 ±18.3	98.0 ±18.3	0.83
FEV ₁ (L)	2.7 ±1.0	2.0 ±0.3	0.041*
FEV ₁ (% predicted)	86.3 ±20.5	86.4 ±15.8	0.99

Data are presented as mean ±SD. Body mass index (BMI); Body surface area (BSA); Peak height velocity (PHV); Forced vital capacity (FVC); Forced expiratory volume in 1 second (FEV₁).

Table 2. Maximal and sub-maximal cardiopulmonary exercise test data

Variable	Male	Female	P value
Sub-maximal			
GET (L/min)	1.03 ±0.25	0.80 ±0.15	0.016*
GET (% VO ₂ peak)	52.56 ±8.19	65.47 ±11.25	0.004*
VE/VCO ₂ slope	31.11 ±4.67	29.21 ±5.35	0.39
Maximal			
VO ₂ peak (L/min)	2.04 ±0.67	1.25 ±0.23	0.002*
Power output peak (W)	174.21 ±70.03	100.80 ±20.24	0.004*
VCO ₂ peak (L/min)	2.47 ±0.80	1.40 ±0.27	0.001*
RER peak	1.25 ±0.98	1.18 ±0.11	0.16
VE peak	81.20 ±25.20	43.28 ±9.10	0.001*

Data are presented as mean ±SD. Gas exchange threshold (GET); Minute ventilation (VE); Oxygen uptake (VO₂); Carbon dioxide production (VCO₂); Respiratory exchange ratio (RER).

Table 3. Sex differences in maximal exercise variables after adjusting for size and covariates

Variable	Males	Females	P value	P adj BMI	P adj FEV1	P adj PHV
VE/VO ₂ peak	41.05 ±8.80	34.92 ±5.31	0.06	0.08	0.06	0.07
VE/VCO ₂ peak	33.60 ± 5.88	31.07 ± 4.65	0.27	0.23	0.15	0.32
Ratio standard method						
VO ₂ /BM	39.57 ± 8.67	33.90 ± 7.54	0.11	0.07	0.08	0.06
VO ₂ /BSA	1276.16 ± 265.45	946.82 ± 119.06	0.001*	0.006*	0.016*	0.001*
VO ₂ /Stature	1258.75 ± 337.70	833.16 ± 119.77	0.001*	0.008*	0.004*	0.001*
Allometrically scaled						
VO ₂ /BM ^{0.77}	91.33 ± 18.15	70.37 ± 9.55	0.003*	0.005*	0.033*	0.002*
VO ₂ /BSA ^{1.2}	1167.28 ± 226.36	898.98 ± 123.80	0.003*	0.005*	0.028*	0.002*
VO ₂ /Stature ^{2.49}	622.44 ± 126.00	462.10 ± 71.74	0.002*	0.010*	0.018*	0.002*

Data are presented as mean ±SD. Minute ventilation (VE); Oxygen uptake (VO₂); Carbon dioxide production (VCO₂); Body mass (BM); Body surface area (BSA); Adjusted (adj).

*p<0.05

CONCLUSION

Exercise capacity is reduced in females with CF when scaled for a range of body size variable and after adjustment for lung function, maturity and BMI.



Future research should explore whether effective training programs for girls with CF can reduce the sex difference in exercise capacity and as a consequence, the possibility of reducing the sex difference in mortality between females and males with CF.

Acknowledgement. This research was undertaken by _____ as part of a summer studentship award from the Cystic Fibrosis Trust. The authors include academic supervisors and researchers who collected the retrospective data as part of previous studies.